ACS OMEGA

Open Access

This article is licensed under CC-BY-NC-ND 4.0

http://pubs.acs.org/journal/acsodf

Article

Study on the Synergistic Suppression Effect and Mechanism of N_2/Ultrafine Water Mist on Liquefied Petroleum Gas Explosion

Bei Pei,* Yuliang Han, Liwei Chen, Ziwei Hu, Zhiqi Wu, Hang Lv, and Wentao Ji

Cite This: *ACS Omega* 2024, 9, 14539−14550

Read Online

ACCESS | Metrics & More | Article Recommendations

ABSTRACT: Liquefied petroleum gas (LPG) is widely used for its cleanliness and high efficiency in industry and city life. In order to improve the suppression effect on LPG explosion, a constant volume combustion bomb was used to investigate the synergistic influence of N_2/ultrafine water mist on the explosion and combustion characteristics of 6% premixed LPG/air gas. The results showed that (1) the effect of a single ultrafine water mist on suppressing LPG explosion is unstable. When the concentration of ultrafine water mist is low, the flame acceleration in the initial stage of explosion is promoted, and when the ultrafine water mist with a mass fraction of 420 g/m^3 is introduced, the maximum pressure rise rate increases. (2) The combination of N_2/ultrafine water mist has a synergistic effect on LPG explosion. Compared to the individual suppression effects, the combination of N_2/ultrafine water mist showed more effective suppression on the explosion pressure, flame propagation, and flame instability of LPG explosion. (3) Through the mechanism analysis, it is found that the combined action of N_2/ ultrafine water mist can better reduce the mole fraction and ROP peak of active free radicals such as H, O, and OH by inhibiting the main reaction of generating H, O, and OH radicals during the explosion of LPG, resulting in the reduction of flame free radicals in the explosion system, thus effectively inhibiting the chain reaction of ignition and explosion of LPG. This research can provide guidance for a better understanding and implementation of gas−liquid two-phase suppression technology for LPG explosion.

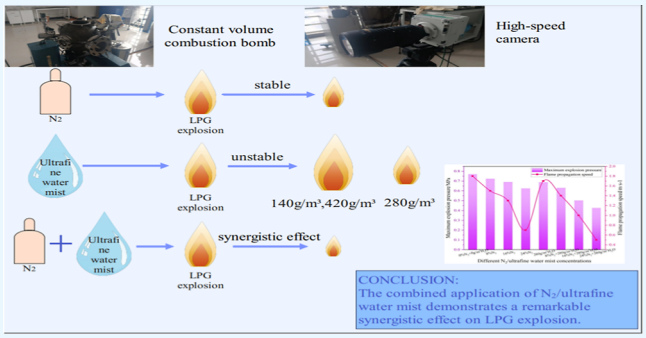

1. INTRODUCTION

Liquefied petroleum gas (LPG) is a basic chemical raw material and clean fuel that is widely used in industrial and civil applications.[1,2] In recent years, under the guidance of the "dual-carbon goal",[3,4] LPG has been further used in production and city life due to its cleanliness and low cost. However, because of the high specific gravity and high chemical activity of LPG, it can easily accumulate in low-lying areas after leakage. Once ignited, it poses a high risk of explosion and combustion accidents. In recent years, both domestic and international incidents involving LPG explosions and fires have occurred with increasing frequency. For instance, the truck tanker accident in India in 2012 resulted in substantial property damage and casualties.[5] In 2020, the "6.13" tanker explosion accident in Wenling caused 20 deaths, and 172 people were hospitalized.[6] Therefore, conducting research on LPG explosion characteristics and explosion suppression techniques holds great significance for industrial and urban safety.

Currently, research on the explosion characteristics of LPG primarily concentrates on the explosion pressure, flame propagation characteristics, and influencing factors. In terms of explosion characteristics, Wang et al.[7] conducted tests on the explosive characteristics of gasoline−air mixtures in a 907.5 L oil tank. They observed that with an increase in gasoline concentration the maximum explosion pressure and maximum pressure rise rate initially increased and then decreased within a certain range. Furthermore, it was noted that the maximum explosion pressure exhibited a linear increasing trend, while the maximum pressure rise rate showed a logarithmic increasing trend with increasing heat energy. Huo and Chow[8] carried out a flame propagation study of an in-tube premixed LPG explosion. Their findings indicated that the flame propagation velocity at the explosion point depends on both the turbulent combustion velocity and the expansion ratio. Razus et al.[9] revealed that the addition of dilution inert gas can mitigate the severity of LPG explosions and decrease the flame front speed by extending the duration of heat loss during combustion. Wang and Liang and Wang et al.[10,11] observed that the addition of hydrogen increased the sensitivity coefficient of reactants C_3H_8 and C_4H_{10}, the maximum ROP of free radicals H, O, and OH, and

Received: January 17, 2024
Revised: February 26, 2024
Accepted: March 1, 2024
Published: March 14, 2024

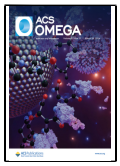

© 2024 The Authors. Published by American Chemical Society

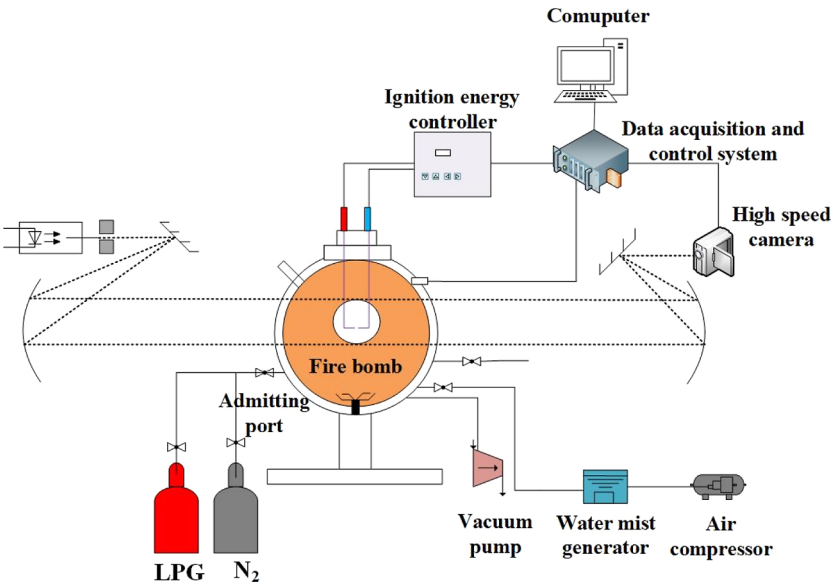

Figure 1. Diagram of experimental equipment.

the explosive strength of the reaction. For the LPG/H_2/air mixture, adding N_2 and CO_2 can inhibit its explosion strength, and the explosion suppression effect of CO_2 is better than that of N_2. It is found by simulation software that the addition of N_2 and CO_2 reduces the maximum ROP of free radicals H, O, and OH. Wang et al.[12] obtained through experiments that repeatedly placing rectangular obstacles increased the maximum explosion pressure and the revised deflagration index, shortened the time to reach the maximum pressure, and significantly elevated the explosion hazard level of LPG−air mixtures.

At present, inert gases such as N_2 and CO_2 are commonly employed in the research on LPG explosion suppression technology. Kai et al.[13] pointed out that both N_2 and CO_2 provide good inhibition of syngas/air explosions. Shang et al.[14] concluded from their experiments that the inhibition effect of CO_2 and N_2 is primarily due to a thermal effect, meaning that the inhibition effect is achieved by reducing the temperature. Li et al.[15] found that CO_2 is obviously superior to N_2 in suppressing the explosion of CH_4- air mixtures in a closed space. Kumar and Mishra et al.[16] observed that the introduction of N_2 resulted in an increase in flame length across all lip thickness, with flame length decreasing as lip thickness increased. Du et al.[17] conducted experimental research on the suppression of nonpremixed gasoline−air mixture explosions in a confined tunnel using N_2. Their results indicated that under nonpremixed suppression conditions, both the maximum pressure value and the rate of pressure rise during the explosion were lower compared to conditions without nonpremixed suppression. Luo et al.[18] discovered that the inclusion of N_2 and CO_2 led to a reduction in the maximum pressure, maximum pressure rise rate, and average flame propagation speed during LPG explosions. Furthermore, they observed that the inerting effect became more pronounced with higher concentrations of these gases. Tu et al.[19] researched the inhibitory effect of N_2 on free radicals in the reaction process by numerical simulation. They discovered that the addition of N_2 significantly reduced the concentration of free radicals, thereby inhibiting the explosion.

Water mist dilution is a common method for suppressing LPG explosions. Water mist is cost-effective and readily accessible.[20] It has no environmental pollution, possesses robust heat absorption and cooling capabilities, and can promptly block and reduce thermal radiation. Additionally, it offers advantages in isolating oxygen and suppressing explosions.[21] As a result, this method has garnered increasing attention from scholars both domestically and internationally. Li et al.[22] found that water mist can significantly reduce the deflagration of propane/air, and the characteristics of the spray and the nozzle's installation position have a significant impact on the explosion-proof effect. Xu et al. and You et al.[23,24] found that the temperature, delay time, flame speed, and overpressure of methane explosions are significantly reduced in the presence of ultrafine water mist. Ananth et al.[25] discovered that the inhibitory effect of fine water mist is primarily due to latent heat absorption, followed by sensible heat absorption by water vapor (and droplets) and momentum absorption by subdroplets into high-velocity gases.

Pei et al.[26−28] found that the combination of inert gas and fine water mist can prevent the explosive phenomenon that may occur with fine water mist alone. The two together exhibit a synergistic inhibitory effect. N_2/ultrafine water mist has a synergistic inhibitory effect on gas explosions, and this inhibitory effect tends to stabilize as the concentration of the N_2/ultrafine water mist increases. Cao et al.[29] found that the addition of NaCl to ultrafine water mist can further enhance the explosion suppression effect. Holborn et al.[30,31] conducted research indicating that the combination of high-density water mist and nitrogen is an effective approach to reduce the explosion intensity of hydrogen, and this combined method outperforms a single water mist.

In summary, it has been observed that the combination of inert gas and ultrafine water mist can significantly enhance the explosion suppression effectiveness for combustible gases, such as methane. However, the literature primarily focuses on single-component combustible gases such as methane and hydrogen. Since LPG consists of propane, butane, and other combustible components and its specific gravity exceeds that of air, it is imperative to investigate the explosion suppression characteristics of gas−liquid two-phase LPG detonation for the safety of the petrochemical industry. This study takes N_2/ultrafine water mist as an example to comparatively examine the suppression characteristics of gas−liquid two-phase explosion suppression

https://doi.org/10.1021/acsomega.4c00555
ACS Omega 2024, 9, 14539−14550

on LPG explosion using a constant volume combustion bomb. Additionally, the reaction mechanism of the N_2/ultrafine water mist was analyzed using CHEMKIN-Pro software. The research findings will offer valuable technical insights for LPG explosion suppression in both petrochemical production and urban domestic gas utilization.

2. EXPERIMENTAL SECTION

2.1. Experimental System. As shown in Figure 1, the experimental setup comprises key components, including a constant volume combustion bomb, a high-speed schlieren system, an ignition system, a gas distribution system, an ultrafine water mist generation and distribution device, a data acquisition system, and a synchronized control system.

The constant volume combustion bomb consists of a double-layer stainless steel sphere with a volume of 20 L and a pressure measurement range of 0−2.0 MPa. The model of the high-speed camera is a Speed Sense VEO 710, the pixel is set to 1280 × 700 resolution, and the shooting frequency is 5000 fps. The schlieren model is CQW300, which is mainly composed of a light source, a slit, a small reflector, a main reflector, and a knife edge. The high-speed camera and schlieren instrument can capture and photograph the explosion flame and analyze the flame propagation characteristics. The ignition system consists of a spark generator and an ignition electrode. In this experiment, the electrode spacing is 3 mm, and the ignition delay time is 100 ms. The gas distribution system consists of an air compressor, gas valve, gas pipe, gas cylinder, GM-240200 mass flow controller (MFC), etc., and the intake is controlled by a computer. The ultrafine water mist generating and conveying system consists of an atomizing device, a sealed square water storage box, a pipeline, etc. The ultrasonic atomizing device adopts a three-head all-copper atomizer, and the working frequency of the atomizing blade is 1700 kHz. After many measurements, the average generation rate of the ultrafine water mist generating system is 11.2 g/min, and the ultrafine water mist is introduced into a constant volume combustion bomb through air. However, gaseous H_2O was used in the CHEMKIN-Pro calculation because liquid H_2O cannot be calculated with CHEMKIN-Pro.[32] The average particle size of ultrafine water mist used in the experiment is 6 μm, which evaporates into a gaseous state during the reaction, so this paper sets ultrafine water mist as gaseous water. The volume fraction of H_2O (CO_2), φ, is defined as

$$\varphi_{H_2O(N_2)} = X_{H_2O(N_2)}/X_{H_2O(N_2)} + X_{LPG} + X_{Air} \quad (1)$$

Here, X refers to the volume of the specific species in the mixtures. The volume of the ultrafine water mist is 10%, and the N_2 volume is 8%.

2.2. Experimental Methods. To analyze the effects of different N_2 and ultrafine water mist concentrations on the explosion as well as the flame propagation characteristics of LPG, the experimental gas was prepared by the China Jiyuan LPG Company. LPG consists of 30% propane and 70% butane by volume. The volume fraction of LPG was set at 6%, setting the N_2 flow rate at 8, 16, and 24% (volume fraction), and the ultrafine water mist flow time at 15, 30, and 45 s. It can be calculated according to the output rate of ultrafine water mist of 11.2 g/min, and the corresponding mass concentrations are 140, 280, and 420 g/m^3. The purity of N_2 reached 99.9%.

During the experiment, the constant volume combustion bomb was first evacuated to negative pressure by using a vacuum pump. Subsequently, LPG and N_2 were introduced sequentially following the Dalton partial pressure method. Ultrafine water mist was introduced into the constant volume combustion bomb along with air, and the intake rate was regulated by a mass flow controller. The introduction time was controlled using the switch on the ultrafine water mist generator, after which the generator was turned off. Finally, air was added to equalize the internal pressure of the constant volume combustion bomb with the atmospheric pressure. Once the gas inlet was completed, the mixture of sample gas and water mist was allowed to stand for 30 s to ensure even mixing. Ignition was computer-controlled, and the pressure acquisition system and picture acquisition system were simultaneously triggered to record the explosion pressure and images. After the experiment, the constant volume combustion bomb was purged with four times the volume of air to remove waste gas and ensure that the container was dry. To guarantee the accuracy of the experimental data, each set of working conditions was repeated five times. All the tests were carried out in the environment of P = 0.1 MPa and T = 298.3 K.

2.3. Data Processing. In this paper, the radius of a spherical flame is calculated by the equal area method.[32,33] The stretched flame propagation velocity, S_n, can be calculated by

$$S_n = dr_u/dt \quad (2)$$

The stretching rate α and the length of Markstein are obtained. The stretch ratio is the derivative of the logarithmic value of an infinitesimal area on a flame with respect to time, and the calculation method is as follows

$$\alpha = d \ln A/dt = 1dA/Adt = 2dr_u/r_u dt = 2S_n/r_u \quad (3)$$

At the initial stage of flame propagation, there is a time when the pressure changes little. At this time, the propagation speed S_n of the stretching flame and the flame stretching rate α can be approximately linear

$$S_l - S_n = L_b\alpha \quad (4)$$

S_l represents the nonstretched flame propagation velocity, and L_b denotes the Markstein length. The Markstein length reflects the flame's sensitivity to stretching, with values less than zero indicating flame instability and values greater than zero indicating flame stability.

3. ANALYSIS AND DISCUSSION

3.1. Influence on LPG Explosion Pressure. *3.1.1. Influence of a Single Inhibitor.* The explosion pressure is a crucial parameter that reflects explosion characteristics, and the rate of pressure rise effectively demonstrates the explosion strength. Figure 2 shows the maximum explosion pressure (P_{max}), time to reach the maximum explosion pressure (t_a), maximum pressure rise rate [$(dP/dt)max$], and time to reach the maximum pressure rise rate (t_b) of 6% LPG exploded by N_2 with different volume fractions. It was observed that as the volume fraction of N_2 increased, both P_{max} and $(dP/dt)_{max}$ gradually decreased, while t_a and t_b gradually increased. This is consistent with previous research results.[18]

Figure 3 depicts the effects of varying concentrations of ultrafine water mist on the P_{max}, t_a, $(dP/dt)_{max}$, and t_b of a 6% LPG explosion. As shown in Figure 3, within the test concentration range, the decrease in P_{max} remains within 20%, and the explosion suppression effect of the ultrafine water mist is inferior to that of N_2. Upon the introduction of 140 and 280 g/m^3 ultrafine water mist, t_a increases by 38.2 and 28.1%, $(dP/dt)_{max}$ decreases by 28.7 and 32.5%, and t_b extends by 32.4 and

https://doi.org/10.1021/acsomega.4c00555
ACS Omega 2024, 9, 14539−14550

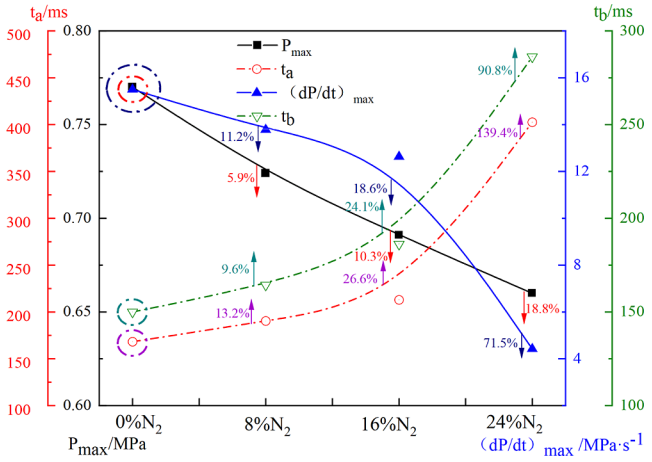

Figure 2. Effects of N_2 on P_{max}, t_a, $(dP/dt)_{max}$ and t_b of 6% LPG explosion.

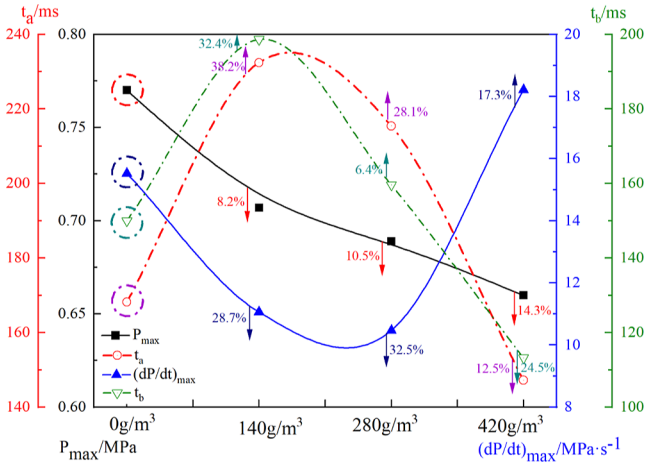

Figure 3. Effects of ultrafine water mist on P_{max}, t_a, $(dP/dt)_{max}$, and t_b of a 6% LPG explosion.

6.4%, respectively. However, when the concentration of ultrafine water mist is further raised to 420 g/m^3, t_a is 12.5% earlier, $(dP/dt)_{max}$ increases by 17.3%, and t_b is 24.5% earlier. Although ultrafine water mist can reduce P_{max}, there is no clear pattern for $(dP/dt)_{max}$, t_a, and t_b, suggesting that the suppression effect of ultrafine water mist on LPG explosion does not improve with increasing mass concentration because the use of a single ultrafine water mist can lead to vapor-pressure-induced explosion suppression instability. Cao et al.[34] demonstrates that steam pressure, as part of the explosion pressure in a closed container, influences the overall explosion pressure.

3.1.2. Influence of N_2/Ultrafine Water Mist Gas−Liquid Two-Phase Inhibitor. To elucidate the impact of N_2/ultrafine water mist on the pressure of a 6% LPG explosion, this study selected the combination of N_2/ultrafine water mist with a mass concentration of 280 g/m^3 for analysis Figure 4 illustrates the effect of N_2/ultrafine water mist on P_{max}, t_a, $(dP/dt)_{max}$, and t_b of 6% LPG. According to Figure 4, when the N_2/ultrafine water mist gas−liquid two-phase explosion suppressant is applied, the explosion suppression effect is significantly enhanced. When 280 g/m^3 of ultrafine water mist is combined with 24% N_2, P_{max} decreases to 0.427 MPa, and t_a extends to 690.8 ms. Compared to the 6% LPG explosion alone, P_{max} and $(dP/dt)_{max}$ decrease by 44.5 and 92.8%, respectively, while t_a and t_b increase by 310.7

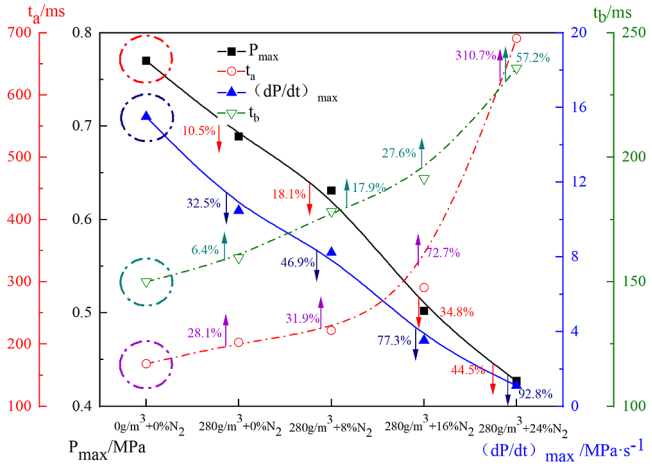

Figure 4. Effects of N_2/ultrafine water mist on P_{max}, t_a, $(dP/dt)_{max}$, and t_b of a 6% LPG explosion.

and 57.2%, respectively. It is evident that when both are combined, the reduction in P_{max} and $(dP/dt)_{max}$ is more pronounced, and ta and t_b experience significant delays. This indicates a synergistic enhancement in the pressure suppression effect of N_2/ultrafine water mist on LPG explosion when used together, surpassing the effect of each as a single inhibitor and avoiding the situation that $(dP/dt)_{max}$ increases and the unstable explosion suppression effect under the condition of a single ultrafine water mist, and its suppression effect on LPG explosion pressure is significantly better than that of a single inhibitor. This improvement is attributed to the prolonged residence time of ultrafine water mist in the flame zone due to N_2 inertization, leading to enhanced evaporation heat absorption, dilution, and a further reduction in combustion rate, resulting in superior LPG explosion suppression.[28]

3.2. Influence on Flame Propagation Characteristics during the Initial Stage of LPG Explosion. When combustible gases burn in enclosed containers, an interaction occurs between pressure wave reflections and the combustion wave, which can alter the flame propagation characteristics. Therefore, it is essential to investigate the impact of detonation suppressants on flame instability during LPG explosions. To thoroughly study the effect of N_2/ultrafine water mist on flame propagation in the early stage of LPG explosion, the change in the flame propagation characteristics in the early stage of flame propagation from the moment of ignition to the moment when the flame develops to the size of the window as well as the moment when the flame is self-accelerating (i.e., the moment when the cellular structure is generated) is analyzed.

3.2.1. Influence of a Single Inhibitor. 3.2.1.1. Flame Propagation Speed. Figures 5 and 6 depict the effects of N_2 and ultrafine water mist on the flame propagation speed of a 6% LPG explosion, respectively. The changes in flame propagation speed during LPG explosions can be divided into two periods: I is the ignition phase, during which the flame accelerates significantly in the initial ignition stage; II is the flame development phase, where the flame expands from the center, forming a spherical flame that spreads outward and gradually fills the entire window. During this phase, the flame speed gradually stabilizes. Concurrently, the flame propagation speed decreases progressively with the increase of the volume fraction of N_2. The flame speed of the 6% LPG explosion eventually stabilizes at approximately 1.8 m/s. However, when 24% N_2 is introduced,

https://doi.org/10.1021/acsomega.4c00555
ACS Omega 2024, 9, 14539−14550

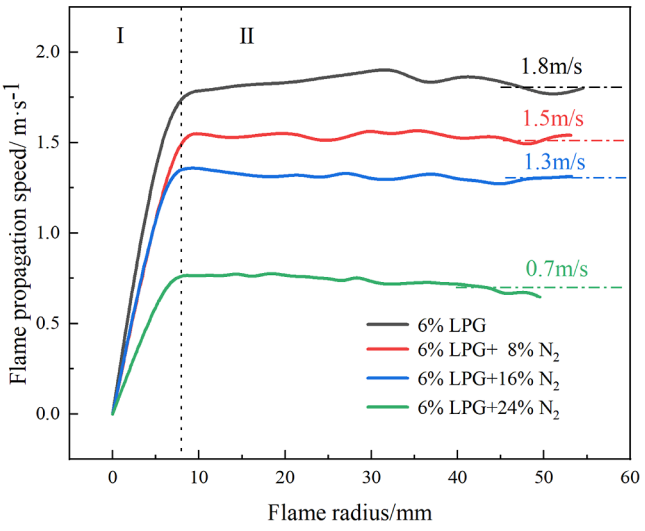

Figure 5. Effects of N_2 on the flame propagation speed of 6% LPG.

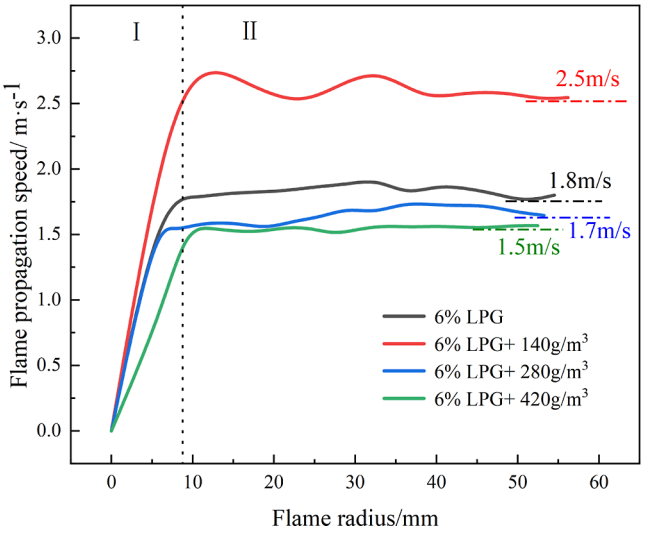

Figure 6. Effects of ultrafine water mist on the flame propagation speed of 6% LPG.

the flame propagation speed significantly decreases and stabilizes at approximately 0.7 m/s, which is 61.1% lower than that of the 6% LPG explosion. This demonstrates that N_2 can reduce the flame propagation speed and inhibit LPG explosions. In contrast, under the influence of ultrafine water mist alone, the flame propagation speed during the LPG explosion does not decrease with increasing concentration. When the concentration of ultrafine water mist is 280 and 420 g/m^3, the flame propagation speed stabilizes at approximately 1.7 and 1.5 m/s, representing only an 5.6 and 16.7% decrease compared to the 6% LPG explosion. However, at concentrations of 140 g/m^3 ultrafine water mist, the flame propagation speed increases and the flame velocity fluctuates significantly. This indicates that the inhibitory effect of a single ultrafine water mist on the flame propagation velocity of LPG is not evident, and its inhibition effect on LPG explosions is unstable.

3.2.1.2. Flame Structure. Figure 7 depicts the spherical flame propagation images of 6% LPG at various moments under the influence of N_2. These images show the ignition time (1 ms), 6 ms, midpoint, time of reaching the edge of the window, formation time of the cell flames, and flame images in the later

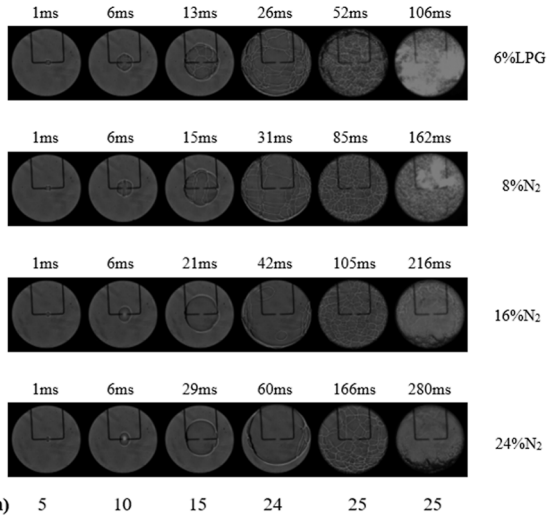

Figure 7. Schlieren image of the effect of N_2 on the 6% LPG explosion flame at different times.

stages of the explosion. Taking the example of a 6% LPG explosion, after ignition, the flame expanded outward in a spherical shape, spreading in a laminar state, with cracks and folds appearing on the flame's surface. At 13 ms, the flame reached the midpoint, with a radius half that of the spherical radius, exhibiting a cellular structure. By 26 ms, the flame reached the edge of the window. Compared to the earlier flame structure, more wrinkles appeared on the flame's surface, and the cellular structure became more pronounced. Large cells gradually differentiated into smaller cells. At 52 ms, a complete cellular structure emerged, and the flame exhibited cellular instability. The surface area of the flame increased, enhancing convection and heat transfer between the flame surface and unburned gas. This led to an increased combustion rate and self-acceleration, ultimately intensifying the explosion. Figure 7 also illustrates the impact of different volume fractions of N_2 on the flame structure of LPG explosions. With the addition of 8% N_2, the time for the flame to reach half of the window extended to 15 ms, and reaching the edge of the window took 31 ms. Complete cells appeared at 85 ms, which shows that 8% N_2 can weaken the flame acceleration in the initial stage of ignition and the initial explosion intensity of LPG.[35] Similarly, when introducing 16 or 24% N_2, the flame arrival time was further delayed, the number of cellular structures decreased, surface wrinkles were reduced, and the flame exhibited slight floating. The suppression effect improved with the increase in the volume fraction of N_2. This indicates that N_2 can inhibit the flame propagation of 6% LPG and reduce its explosion intensity.

Figure 8 displays schlieren images of the spherical flame propagation of a 6% LPG explosion at various times under the influence of an ultrafine water mist. In comparison to a single N_2, the impact of ultrafine water mist on the cellular structures is less pronounced. When 280 and 420 g/m^3 ultrafine water mist was introduced, the flame exhibited a delay, and the number of cell structures decreased. However, with the introduction of 140 g/m^3 ultrafine water mist, the flame reached each stage earlier, indicating acceleration of the flame and intensified flame propagation. This further suggests that the influence of a single ultrafine water mist on the explosion flame structure is unstable, and when the amount of ultrafine water mist is insufficient, it promotes flame propagation.

https://doi.org/10.1021/acsomega.4c00555
ACS Omega 2024, 9, 14539−14550

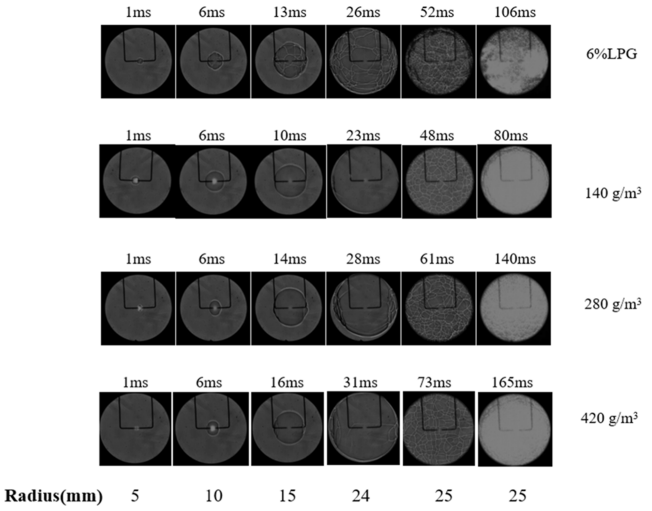

Figure 8. Schlieren image of the effect of ultrafine water mist on the 6% LPG explosion flame at different times.

3.2.1.3. Flame Acceleration Characteristics. According to Figure 9, when the volume fraction of N_2 is 8, 16, and 24%, the unstretched flame propagation speed of LPG at the initial stage of the explosion decreases to 1.55, 1.34, and 0.75 m/s, respectively. As the volume fraction of N_2 increases, the range of flame elongation gradually narrows and the Markstein length increases. The Markstein length of the 6% LPG explosion flame was 0.11 mm, and after adding 8, 16, and 24% N_2, the Markstein length increased to 0.20, 0.35, and 0.59 mm, representing increases of 81.8, 218.2, and 436.4%, respectively. This indicates that N_2 has a significant inhibitory effect on the flame propagation of LPG explosion, and the inhibitory effect increases with the increase of the volume fraction of N_2.

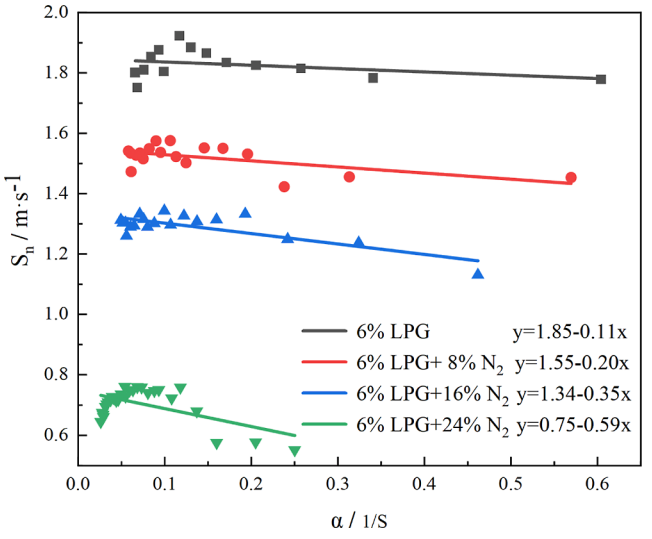

Figure 9. Relationship between flame propagation speed and elongation under different volume fraction of N_2.

3.2.2. Impact of N_2/Ultrafine Water Mist Gas–Liquid Two-Phase Inhibitor. 3.2.2.1. Flame Propagation Speed. Figure 10 illustrates the impact of N_2/ultrafine water mist on the flame propagation speed of a 6% LPG explosion. It is evident that when they are used in conjunction, the flame propagation speed decreases more significantly in comparison to using N_2 or ultrafine water mist as standalone inhibitors. When 24% N_2 and 280 g/m^3 ultrafine water mist are introduced, the flame propagation speed stabilizes at approximately 0.5 m/s, which is 69% lower than that of a pure 6% LPG explosion. A comprehensive comparison reveals that the N_2/ultrafine water mist exhibits a synergistic effect in reducing the flame propagation speed of a 6% LPG explosion.

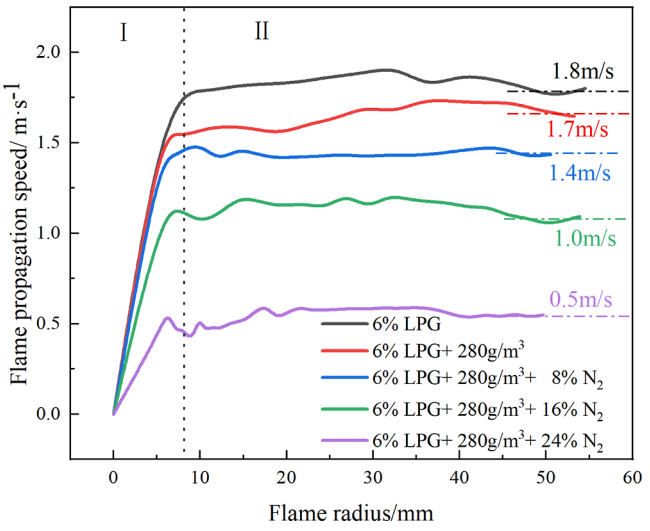

Figure 10. Effects of the N_2/ultrafine water mist on the flame propagation speed of a 6% LPG explosion.

3.2.2.2. Flame Structure. N_2 and 280 g/m^3 ultrafine water mist were selected to act together to further analyze the effect of two-phase inhibitors on the flame structure in the early stage of LPG explosion. The flame propagation images shown in Figure 11 reveal that when used in combination, N_2/ultrafine water mist results in a further reduction in flame propagation speed and delayed arrival times at various stages compared to using N_2 or 280 g/m^3 ultrafine water mist alone. In the case of 24% N_2 and 280 g/m^3 ultrafine water mist used together, for instance, when 24% N_2 or 280 g/m^3 ultrafine water mist is applied alone, the flame reaches the edge of the window in 60 and 28 ms,

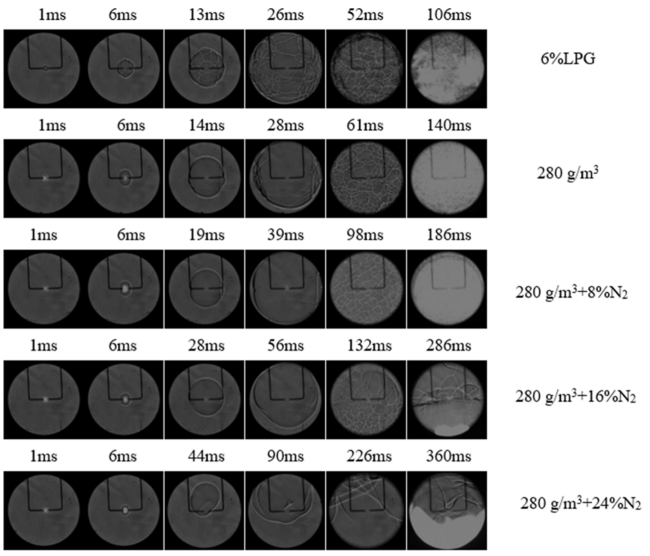

Figure 11. Schlieren image and the effect of N_2/ultrafine water mist on the 6% LPG explosion flame at different times.

https://doi.org/10.1021/acsomega.4c00555
ACS Omega 2024, 9, 14539−14550

respectively. The fullest cellular structure appeared at 166 and 61 ms, respectively. When both are used together, the flame arrival at the edge of the window is extended to 90 ms, the flame cellular structure essentially disappears, and the flame exhibits a floating phenomenon. The self-acceleration phenomenon of the flame in the initial stage of ignition is further weakened with the increase of volume fraction of N_2, thus reducing the initial explosion intensity of LPG explosion, enabling the ultrafine water mist to better play its physical heat absorption and chemical explosion suppression functions,[35] and avoiding the influence of a single ultrafine water mist on the flame structure.

3.2.2.3. Flame Acceleration Characteristics. According to Figure 12, under the combined effect of N_2/ultrafine water mist,

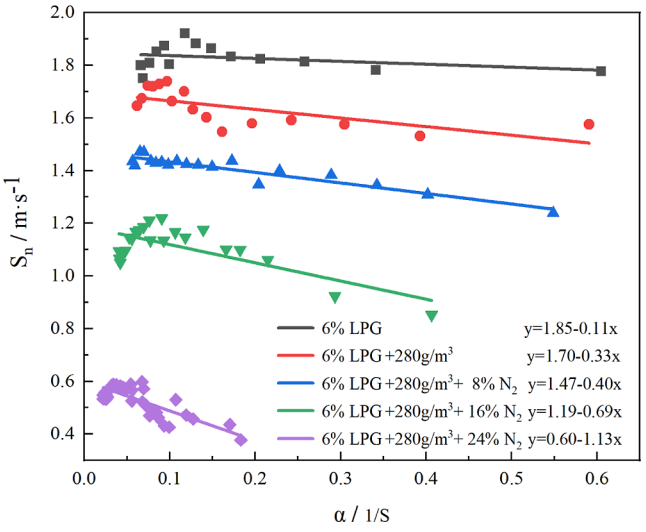

Figure 12. Relationship between flame propagation velocity and elongation under different N_2/ultrafine water mist concentrations.

the flame propagation speed gradually decreases, the flame stretch rate gradually decreases, and the corresponding stretch rate range gradually narrows. Additionally, the Markstein length shows an increasing trend. Compared to a single inhibitor, two-phase inhibitors have the most significant impact on increasing the Markstein length. When 8, 16, 24% N_2, and 280 g/m^3 of ultrafine water mist are combined, the unstretched flame propagation velocity decreases to 1.47, 1.19, and 0.60 m/s, respectively. Furthermore, the Markstein length increases to 0.40 0.69, and 1.13 mm, respectively. Compared to 6% LPG, the Markstein length increases by 263.6, 527.3, and 927.3%, respectively, which is a greater increase than that achieved with a single inhibitor. This indicates that the combined application of N_2/ultrafine water mist is more effective in suppressing flame instability during the initial stages of LPG explosion compared to using a single inhibitor. This observation aligns with the results analyzed from the flame structure images above.

3.3. Analysis of Synergistic Effects. Table 1 provides a comprehensive comparison of the synergistic suppression effect of N_2/ultrafine water mist on 6% LPG explosions. From Table 1, it is evident that compared to the effect of a single inhibitor, the gas−liquid two-phase inhibitor demonstrates a more significant suppression effect on explosion pressure, with larger reductions in P_{max} and $(dP/dt)_{max}$. Simultaneously, there is a greater decrease in flame propagation speed and a more substantial increase in Markstein length, indicating a more pronounced effect on enhancing flame stability. In summary, N_2/ultrafine water mist exhibits a synergistic effect on suppressing LPG explosions, and their combined action results in superior explosion suppression. Taking 16% N_2 and 280 g/m^3 ultrafine water mist as an example. P_{max} decreased by 10.3 and 10.5% when N_2 or ultrafine water mist acted alone but decreased by 34.8% when they were employed together, which was higher than the sum of the two reduction ranges. t_a was extended by 72.7%, while the extension ranges of single N_2 and ultrafine water mist were 26.6 and 28.1%, respectively. $(dP/dt)_{max}$ also shows the same law; under the combined application of N_2/ultrafine water mist, $(dP/dt)_{max}$ decreases by 77.3%, while the decreasing ranges of single N_2 or ultrafine water mist are 18.6 and 32.5%, respectively, which are greater than the sum of the decreasing ranges of N_2/ultrafine water mist. N_2 and ultrafine water mist have obvious synergistic effects on P_{max} and $(dP/dt)_{max}$. Similarly, the combined application of a N_2/ultrafine water mist has a synergistic effect on reducing the flame propagation speed and increasing the Markstein length. When N_2 ultrafine water mist is employed together, the flame propagation speed decreases by 44.4%, while when N_2 or ultrafine water mist is used alone, the decreases are 27.8 and 5.6%, respectively, which is greater than the sum of the decreases under the action of a single inhibitor, and the Markstein length increases by 527.3%, while when N_2 or ultrafine water mist is used alone, the decreases are 218.2 and 200%, respectively, which is greater than the sum of the increases under the action of a single inhibitor.

Table 1. Changes in Explosion Parameters under the Action of a N_2/Ultrafine Water Mist

inhibitory composition	variation range of P_{max}/%	variation range of t_a/%	variation range of $(dP/dt)_{max}$/%	variation range of t_b/%	variation range of flame propagation speed/%	variation range of Markstein length/%
0						
8% N_2	−5.9	+13.2	−11.2	+9.6	−16.7	+81.8
16% N_2	−10.3	+26.6	−18.6	+24.1	−27.8	+218.2
24% N_2	−18.8	+139.4	−71.5	+90.8	−61.1	+436.4
140 g/m^3 H_2O	−8.2	+38.2	−28.7	+32.4	+38.9	
280 g/m^3 H_2O	−10.5	+28.1	−32.5	+6.4	−5.6	+200.0
420 g/m^3 H_2O	−14.3	−12.5	+17.3	−24.5	−16.7	
8% N_2 + 280 g/m^3 H_2O	−18.1	+31.9	−46.9	+17.9	−22.2	+263.6
16% N_2 + 280 g/m^3 H_2O	−34.8	+72.7	−77.3	+27.6	−44.4	+527.3
24% N_2 + 280 g/m^3 H_2O	−44.5	+310.7	−92.8	+57.2	−72.2	+927.3

https://doi.org/10.1021/acsomega.4c00555
ACS Omega 2024, 9, 14539−14550

Table 2. Main Reaction Steps and Basic Reactions of Free Radical Concentration

reaction step	basic reaction	reaction step	basic reaction
R1	$O_2 + H \Leftrightarrow O + OH$	R2	$O + H_2 \Leftrightarrow H + OH$
R3	$OH + H_2 \Leftrightarrow H + H_2O$	R4	$2OH \Leftrightarrow O + H_2O$
R16	$HO_2 + H \Leftrightarrow 2OH$	R31	$OH + CO_2 \Leftrightarrow CO_2 + H$
R40	$HCO + H_2O \Leftrightarrow CO + H + H_2O$	R59	$O_2 + CH_2 \Leftrightarrow HCO + OH$
R88	$CH_3 + H(+M) \Leftrightarrow CH_4(+M)$	R89	$CH_3 + O \Leftrightarrow H + CH_2O$
R123	$CH_4 + H \Leftrightarrow CH_3 + H_2$	R124	$CH_4 + O \Leftrightarrow CH_3 + OH$
R125	$OH + CH_4 \Leftrightarrow CH_3 + H_2O$	R149	$O_2 + HCCO \Leftrightarrow OH + 2CO$
R155	$C_2H_3(+M) \Leftrightarrow C_2H_2 + H(+M)$	R157	$C_2H_2 + O \Leftrightarrow CH_2 + CO$
R158	$C_2H_2 + O \Leftrightarrow H + HCCO$	R249	$C_2H_4 + H(+M) \Leftrightarrow C_2H_5(+M)$
R284	$C_2H_4 + H \Leftrightarrow C_2H_3 + H_2$	R251	$C_2H_4 + O \Leftrightarrow C_2H_3 + OH$
R252	$C_2H_4 + O \Leftrightarrow CH_3 + HCO$	R254	$C_2H_4 + OH \Leftrightarrow C_2H_3 + H_2O$
R631	$C_4H_{10} + H \Leftrightarrow sC_4H_9 + H_2$		

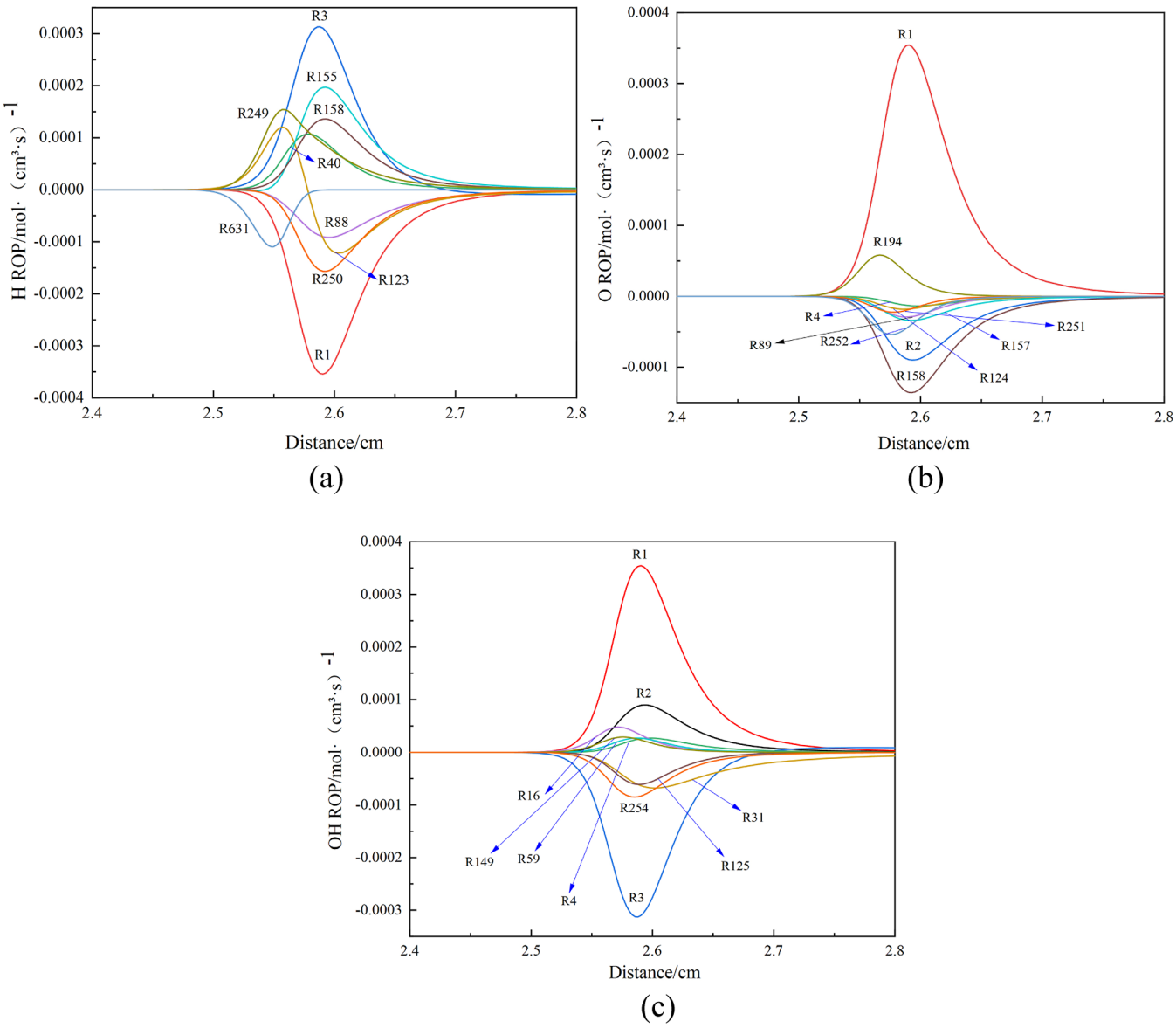

Figure 13. ROP of H, O, and OH radicals in each reaction step: (a) ROP of H radicals; (b) ROP of O radicals; and (c) ROP of OH radicals.

4. ANALYSIS OF INHIBITION MECHANISMS

In order to explore the principle, N_2/ultrafine water mist combined suppression effect on LPG explosion. Utilizing CHEMKIN-Pro simulation software, a simulation study was conducted using the laminar combustion calculation module to simulate the explosion of C_3H_8 and C_4H_{10} (the main components of LPG, the ratio is 3:7) gas mixtures under the impact of N_2/ultrafine water mist. The reaction kinetic mechanism used in this study is GRI Mech3.0, which

https://doi.org/10.1021/acsomega.4c00555
ACS Omega 2024, 9, 14539−14550

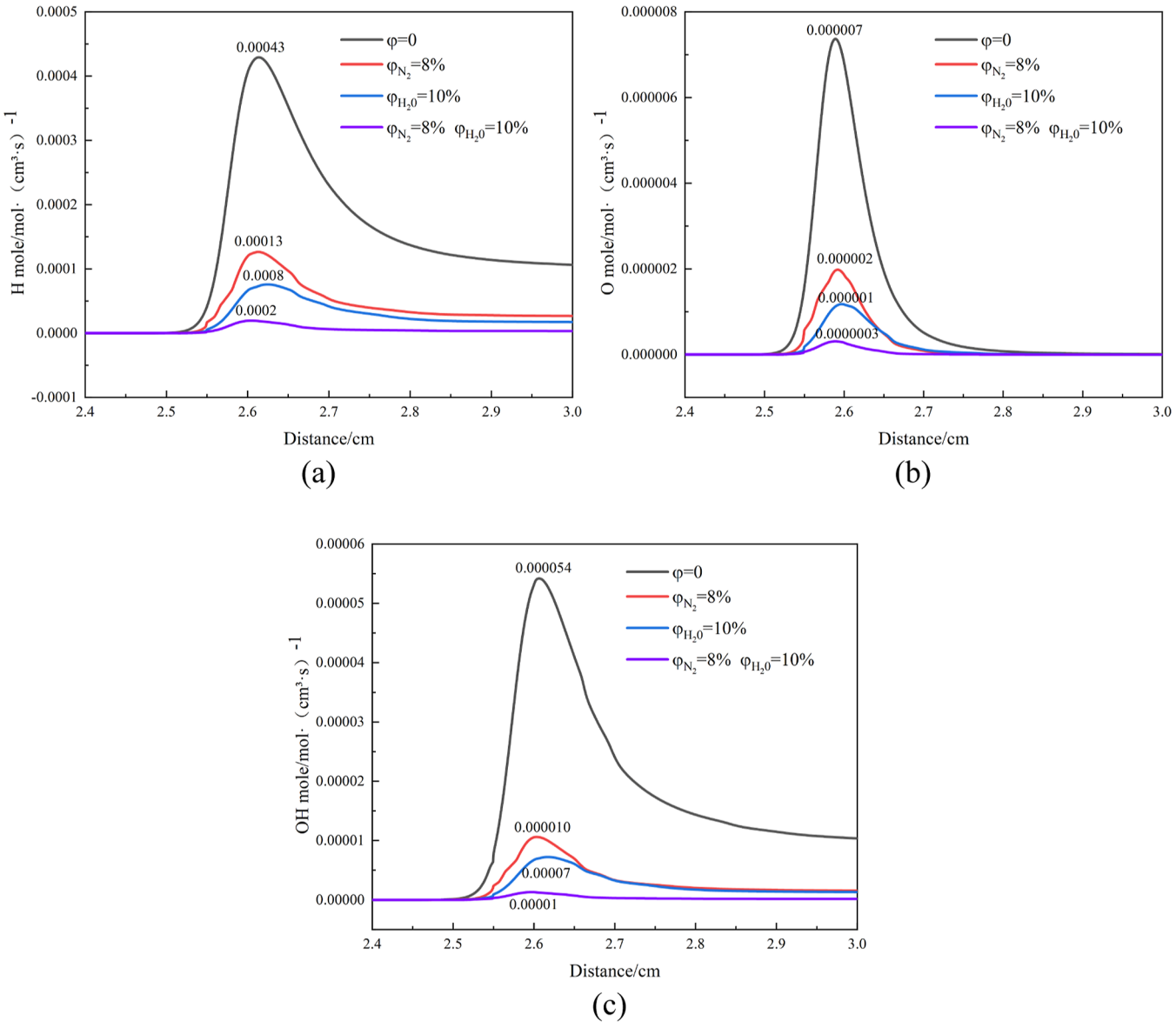

Figure 14. Molar fraction of H/O/OH radicals under different volume fractions of N_2 and H_2O: (a) ROP of H radicals; (b) ROP of O radicals; and (c) ROP of OH radicals.

encompasses 53 components and 325 elementary reactions. Table 2 lists the primitive reactions corresponding to the reaction steps shown in Figure 13. Previous studies have shown that this reaction kinetics mechanism is superior to other reaction models and can elucidate the influence of elementary reactions on the reactants during the reaction process.[32] However, due to the complexity of analyzing all elementary reactions, this paper focuses on analyzing the key elementary reactions.

Gas combustion and explosion are essentially complex chain reactions, in which the free radicals H, O, and OH play an important role, especially in the induction period of gas explosion.[36] Figure 13 illustrates the ROP of H, O, and OH radicals at each reaction step during LPG explosions. In Figure 13a, the most critical basic reactions for H radicals are R3: OH + H_2 <=> H + H_2O and R1: H + O_2 <=> O + OH. R3 is the primary reaction for H radical generation, while R1 is the main reaction for H radical consumption. Conversely, Figure 13c shows that OH radicals exhibit the opposite behavior; R3 is the main reaction for OH radical consumption, and R1 is the primary reaction for OH radical generation. In Figure 13b, for O radicals, R1 is the main reaction for the generation of O radicals, while R158: C_2H_2+O <=> HCCO + H becomes the primary reaction for O radical depletion.

Figures 14 and 15 depict the changes in the molar fractions of H, O, and OH radicals as well as the ROP following the introduction of N_2/ultrafine water mist, respectively. When N_2 or ultrafine water mist is added, fundamental reactions involving the generation and consumption of H, O, and OH radicals remain unchanged. However, the molar fractions of H, O, and OH radicals decrease, indicating that the addition of N_2 or ultrafine water mist can impede the generation of H, O, and OH radicals. This is due to a decrease in the ROP peak of the main reactions R3 and R1, which produce H, O, and OH. Therefore, in this paper, the influence of N_2/ ultrafine water mist on explosive chain reactions of C_3H_8 and C_4H_{10} was analyzed by comparing the molar fraction of H, O, and OH radicals and the change of ROP peak value in the basic reaction. When N_2/

https://doi.org/10.1021/acsomega.4c00555
ACS Omega 2024, 9, 14539−14550

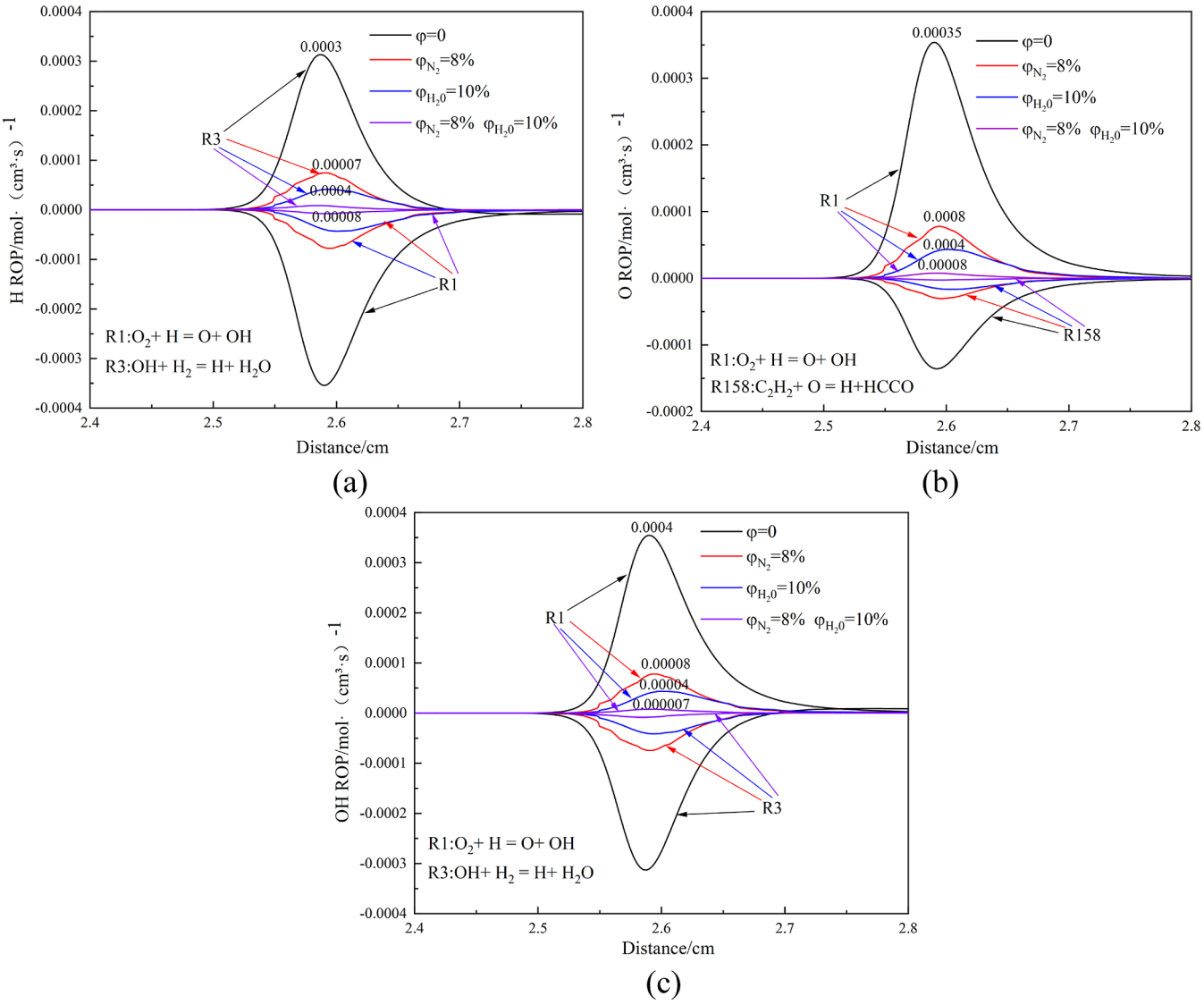

Figure 15. ROP of H, O, and OH radicals after N_2 and H_2O: (a) ROP of H radicals; (b) ROP of O radicals; and (c) ROP of OH radicals.

ultrafine water mist is introduced, a significant decrease in the molar fractions of H, O, and OH radicals is observed. Furthermore, the effect of adding N_2/ultrafine water mist in reducing the molar fractions of H, O, and OH radicals is notably superior to that of adding a single N_2 or ultrafine water mist. This demonstrates that N_2/ultrafine water mist exhibits a synergistic inhibitory effect, better suppressing the generation of H, O, and OH radicals, better reducing the ignition sensitivity of LPG and preventing the explosive chain reaction. This also explains why the explosion parameters are significantly reduced when N2/ ultrafine water mist works synergistically.

5. CONCLUSIONS

In this study, the synergistic inhibition of N_2/ultrafine water mist on a 6% LPG explosion was studied in a constant volume combustion bomb. The inhibition mechanism was analyzed with CHEMKIN-Pro software, and the main conclusions were as follows:

(1) The inhibitory effect of a single ultrafine water mist on LPG explosion was unstable. When 140 g/m^3 ultrafine water mist is introduced, compared with pure LPG explosion, the flame propagation speed is accelerated, the flame stability is reduced, the flame cell structure is more obvious, and the time to reach the end of the window is advanced. When 420 g/m^3 ultrafine water mist is introduced, the maximum pressure rise rate is increased by 17.3% compared with 6% LPG explosion. This is because the single ultrafine water mist is greatly influenced by the vapor pressure formed by the evaporation of water mist, so it cannot play a stable inhibitory effect on LPG explosion.

(2) The combined application of N_2/ultrafine water mist demonstrates a remarkable synergistic effect, the decrease of explosion pressure of LPG by both inhibitors is greater than the sum of the decrease of single inhibitor. In addition, with the increase of volume fraction of N_2, both the maximum explosion pressure and the maximum pressure rise rate decrease significantly, and the arrival time is prolonged.

(3) When N_2/ultrafine water mist is combined, the reduction in flame propagation speed and the increase in the Markstein length are significantly more pronounced compared to the effect of a single inhibitor, and the flame exhibits a noticeable upward movement. This is

https://doi.org/10.1021/acsomega.4c00555
ACS Omega 2024, 9, 14539−14550

because the addition of N_2 weakens the acceleration phenomenon of flame in the initial stage of ignition and weakens the initial explosion intensity of LPG, thus prolonging the action time of ultrafine water mist, improving its explosion suppression effect and avoiding the explosion promotion phenomenon caused by steam pressure when a single ultrafine water mist acts.

(4) Through mechanism analysis, it can be concluded that when N_2/ ultrafine water mist is used in combination, it shows more obvious inhibition on the generation of H, O, and OH free radicals. This is because N_2/ ultrafine water mist can better inhibit the main reactions of generating H, O, and OH radicals by LPG explosion, thus inhibiting the molar fraction and ROP peak of H, O, and OH radicals. Therefore, the total amount of flame free radicals in the explosion system is significantly reduced, which leads to a significant improvement in explosion mitigation efficiency.

AUTHOR INFORMATION

Corresponding Author

Bei Pei − *State Collaborative Innovation Center of Coal Work Safety and Clean-efficiency Utilization, Henan Polytechnic University, Jiaozuo, Henan 454003, PR China*; Email: pb128@hpu.edu.cn

Authors

Yuliang Han − *State Collaborative Innovation Center of Coal Work Safety and Clean-efficiency Utilization, Henan Polytechnic University, Jiaozuo, Henan 454003, PR China*; orcid.org/0009-0009-4496-2379

Liwei Chen − *State Collaborative Innovation Center of Coal Work Safety and Clean-efficiency Utilization, Henan Polytechnic University, Jiaozuo, Henan 454003, PR China*

Ziwei Hu − *State Collaborative Innovation Center of Coal Work Safety and Clean-efficiency Utilization, Henan Polytechnic University, Jiaozuo, Henan 454003, PR China*

Zhiqi Wu − *State Collaborative Innovation Center of Coal Work Safety and Clean-efficiency Utilization, Henan Polytechnic University, Jiaozuo, Henan 454003, PR China*

Hang Lv − *State Collaborative Innovation Center of Coal Work Safety and Clean-efficiency Utilization, Henan Polytechnic University, Jiaozuo, Henan 454003, PR China*

Wentao Ji − *State Collaborative Innovation Center of Coal Work Safety and Clean-efficiency Utilization, Henan Polytechnic University, Jiaozuo, Henan 454003, PR China*; orcid.org/0000-0002-2085-7007

Complete contact information is available at: https://pubs.acs.org/10.1021/acsomega.4c00555

Notes

The authors declare no competing financial interest.

ACKNOWLEDGMENTS

This paper was financially supported by the research fund provided by the Science & Technology Innovation Talents in Universities of Henan Province (no. 22HASTIT027) and Scientific and Technological Key Project of Henan Province (no. 222102320142).

REFERENCES

(1) Troncoso, K.; Segurado, P.; Aguilar, M.; Soares Da Silva, A. Adoption of LPG for cooking in two rural communities of Chiapas, Mexico. *Energy Policy* **2019**, *133*, 110925.

(2) Sharma, A.; Parikh, J.; Singh, C. Transition to LPG for cooking: A case study from two states of India. *Energy Sustainable Dev.* **2019**, *51*, 63−72.

(3) Xu, Y.; Zhao, H. Study on the Environmental Costs of Petrochemical Enterprises Based on Double Carbon Targets. *Environ. Resour. Ecol. J.* **2022**, *6* (5), 90.

(4) Zhou, Z.; Liu, Y.; Du, J. Analysis on the constraint mechanism of transportation carbon emissions in the Pearl River Delta based on 'Dual carbon' goals. *Syst. Sci. Control Eng.* **2022**, *10* (1), 854−864.

(5) Bariha, N.; Mishra, I. M.; Srivastava, V. C. Fire and explosion hazard analysis during surface transport of liquefied petroleum gas (LPG): A case study of LPG truck tanker accident in Kannur, Kerala, India. *J. Loss Prev. Process Ind.* **2016**, *40*, 449−460.

(6) Lyu, S.; Zhang, S.; Huang, X.; Peng, S.; Li, J. Investigation and modeling of the LPG tank truck accident in Wenling, China. *Process Saf. Environ. Prot.* **2022**, *157*, 493−508.

(7) Wang, S.; Wu, D.; Guo, H.; Li, X.; Pu, X.; Yan, Z.; Zhang, P. Effects of concentration, temperature, ignition energy and relative humidity on the overpressure transients of fuel-air explosion in a medium-scale fuel tank. *Fuel* **2020**, *259*, 116265.

(8) Huo, Y.; Chow, W. K. Flame propagation of premixed liquefied petroleum gas explosion in a tube. *Appl. Therm. Eng.* **2017**, *113*, 891−901.

(9) Razus, D.; Brinzea, V.; Mitu, M.; Oancea, D. Burning Velocity of Liquefied Petroleum Gas (LPG)-Air Mixtures in the Presence of Exhaust Gas. *Energy Fuels* **2010**, *24* (3), 1487−1494.

(10) Wang, J.; Liang, Y. Effect of hydrogen on explosion characteristics of liquefied petroleum gas-air mixtures. *Int. J. Hydrogen Energy* **2022**, *47* (6), 4255−4263.

(11) Wang, J.; Liang, Y.; Zhao, Z. Effect of N_2 and CO_2 on explosion behavior of H2-Liquefied petroleum gas-air mixtures in a confined space. *Int. J. Hydrogen Energy* **2022**, *47* (56), 23887−23897.

(12) Wang, T.; Yi, W.; Liang, H.; Yang, P.; Luo, Z.; Sun, L.; Cheng, F.; Kang, X.; Feng, Z.; Deng, J. Experimental research on the pressure and flame propagation behaviors of LPG-air mixtures in a double obstructed tube. *J. Loss Prev. Process Ind.* **2023**, *82*, 104979.

(13) Kai, Z.; Xufeng, Y.; Minggao, Y.; Rongjun, S.; Lei, W., Effect of N_2 and CO_2 on explosion behavior of syngas/air mixtures in a closed duct. **2019**,.

(14) Shang, R.; Zhang, Y.; Zhu, M.; Zhang, Z.; Zhang, D.; Li, G. Laminar flame speed of CO_2 and N_2 diluted H_2/CO/air flames. *Int. J. Hydrogen Energy* **2016**, *41* (33), 15056−15067.

(15) Li, M.; Xu, J.; Wang, C.; Wang, B. Thermal and kinetics mechanism of explosion mitigation of methane-air mixture by N_2/CO_2 in a closed compartment. *Fuel* **2019**, *255*, 115747.

(16) Kumar, P.; Mishra, D. P. Characterization of bluff-body stabilized LPG jet diffusion flame with N_2 dilution. *Energy Convers. Manage.* **2008**, *49* (10), 2698−2703.

(17) Du, Y.; Zhang, P.; Zhou, Y.; Wu, S.; Xu, J.; Li, G. Suppressions of gasoline-air mixture explosion by non-premixed nitrogen in a closed tunnel. *J. Loss Prev. Process Ind.* **2014**, *31*, 113−120.

(18) Luo, Z.; Wei, C.; Wang, T.; Su, B.; Cheng, F.; Liu, C.; Wang, Y. Effects of N_2 and CO_2 dilution on the explosion behavior of liquefied petroleum gas (LPG)-air mixtures. *J. Hazard. Mater.* **2021**, *403*, 123843.

(19) Tu, Y.; Xu, M.; Zhou, D.; Wang, Q.; Yang, W.; Liu, H. CFD and kinetic modelling study of methane MILD combustion in O_2/N_2, O_2/CO_2 and O_2/H_2O atmospheres. *Appl. Energy* **2019**, *240*, 1003−1013.

(20) Grant, G.; Brenton, J.; Drysdale, D. Fire suppression by water sprays. *Prog. Energy Combust. Sci.* **2000**, *26* (2), 79−130.

(21) Yang, K.; Zhang, P.; Yue, C.; Chen, K.; Ji, H.; Xing, Z.; Hao, Y.; Jiang, J. Experimental research on methane/air explosion inhibition using ultrafine water mist containing methane oxidizing bacteria. *J. Loss Prev. Process Ind.* **2020**, *67*, 104256.

(22) Li, G.; Pan, C.; Liu, Y.; Zhu, X.; Ni, X.; Zhao, X.; Chen, G.; Wang, X. Evaluation of the effect of water mist on propane/air mixture deflagration: Large-scale test. *Process Saf. Environ. Prot.* **2021**, *147*, 1101−1109.
(23) Xu, H.; Li, Y.; Zhu, P.; Wang, X.; Zhang, H. Experimental study on the mitigation via an ultra-fine water mist of methane/coal dust mixture explosions in the presence of obstacles. *J. Loss Prev. Process Ind.* **2013**, *26* (4), 815−820.
(24) You, H.; Yu, M.; Zheng, L.; An, A. Study on Suppression of the Coal Dust/Methane/Air Mixture Explosion in Experimental Tube by Water Mist. *Procedia Eng.* **2011**, *26* (C), 803−810.
(25) Ananth, R.; Willauer, H. D.; Farley, J. P.; Williams, F. W. Effects of Fine Water Mist on a Confined Blast. *Fire Technol.* **2012**, *48* (3), 641−675.
(26) Pei, B.; Yang, Y.; Li, J.; Yu, M. Experimental Study on Suppression Effect of Inert Gas Two Fluid Water Mist System on Methane Explosion. *Procedia Eng.* **2018**, *211*, 565−574.
(27) Pei, B.; Yu, M.; Chen, L.; Zhu, X.; Yang, Y. Experimental study on the synergistic inhibition effect of nitrogen and ultrafine water mist on gas explosion in a vented duct. *J. Loss Prev. Process Ind.* **2016**, *40*, 546−553.
(28) Pei, B.; Li, J.; Wang, Y.; Wen, X.; Yu, M.; Jing, G. Synergistic inhibition effect on methane/air explosions by N_2-twin-fluid water mist containing sodium chloride additive. *Fuel* **2019**, *253*, 361−368.
(29) Cao, X.; Ren, J.; Zhou, Y.; Wang, Q.; Gao, X.; Bi, M. Suppression of methane/air explosion by ultrafine water mist containing sodium chloride additive. *J. Hazard. Mater.* **2015**, *285*, 311−318.
(30) Holborn, P. G.; Battersby, P.; Ingram, J. M.; Averill, A. F.; Nolan, P. F. Estimating the effect of water fog and nitrogen dilution upon the burning velocity of hydrogen deflagrations from experimental test data. *Int. J. Hydrogen Energy* **2013**, *38* (16), 6882−6895.
(31) Holborn, P. G.; Battersby, P.; Ingram, J. M.; Averill, A. F.; Nolan, P. F. Modelling the mitigation of hydrogen deflagrations in a vented cylindrical rig with water fog and nitrogen dilution. *Int. J. Hydrogen Energy* **2013**, *38* (8), 3471−3487.
(32) Wei, S.; Yu, M.; Pei, B.; Zhu, Z.; Zhang, Z. Suppression of CO_2 and H_2O on the cellular instability of premixed methane/air flame. *Fuel* **2020**, *264*, 116862.
(33) Xu, C.; Zhong, A.; Wang, H.; Jiang, C.; Sahu, A.; Zhou, W.; Wang, C. Laminar burning velocity of 2-methylfuran-air mixtures at elevated pressures and temperatures: Experimental and modeling studies. *Fuel* **2018**, *231*, 215−223.
(34) Cao, X.; Wang, Z.; Lu, Y.; Wang, Y. Numerical simulation of methane explosion suppression by ultrafine water mist in a confined space. *Tunn. Undergr. Space Technol.* **2021**, *109*, 103777.
(35) Pei, B.; Yu, M.; Chen, L.; Wang, F.; Yang, Y.; Zhu, X. Experimental study on the synergistic inhibition effect of gas-liquid two phase medium on gas explosion. *J. Loss Prev. Process Ind.* **2017**, *49*, 797−804.
(36) Zhou, S.; Gao, J.; Luo, Z.; Hu, S.; Wang, L.; Wang, T. Role of ferromagnetic metal velvet and DC magnetic field on the explosion of a C_3H_8/air mixture-effect on reaction mechanism. *Energy* **2022**, *239*, 122218.

https://doi.org/10.1021/acsomega.4c00555
ACS Omega 2024, 9, 14539−14550